MECHANIKA
TEORETYCZNA
I STOSOWANA
2/3, 21 (1983)

APPLICATION OF THE MOIRÉ METHOD TO THE ANALYSIS OF FAILURE MODES OF METAL STRIPS

CEZARY AJDUKIEWICZ

Politechnika Warszawska

PRZEMYSŁAW JASTRZĘBSKI

Politechnika Warszawska

1. Introductory remarks

Since the exact determination of the limit load of structural elements is often difficult and sometimes even impossible it is the upper or the lower bound assesment, based on the extremum principles of the theory of plasticity, that is commonly regarded as satisfactory. The lower bound to the external forces causing plastic flow is obtained by assuming such a statically admissible stress field in an element which gives the highest possible loadcarrying capacity. The upper bound is obtained by assuming such a kinematically admissible deformation mechanism which gives the lowest possible load — carrying capacity.

In the latter approach the estimation of the limit load of structural elements depends largely on assuming the proper kinematically admissible deformation mechanism. Thus, the experimental verification of theoretical solutions is of particular interest. The frequently used method of etching (see [3]) has a disadvantage of showing only fully developed slipline patterns. This fact together with a certain amount of freedom in image interpretation makes the determination of the proper failure mode rather un — reliable. A layer of ferro — ferric oxide deposited during the metallurgical processing on the surface of rolled elements such as sheet metal forms a natural brittle coating which sometimes can be used effectively. However, specimens made of such materials are not always available. The method of photoelastic coating is, in turn, mainly applied to the investigation of propagation of plastic zones (see [4]).

In this paper an application will be proposed of the moiré method [6] for the determination of failure modes in plane elements. The advantage of the method consists in a possibility of observation of sliplines development almost from the beginning of their formation.

2. Experimental investigations

A characteristic moiré fringe pattern (fig. 1) can be observed on the surface of mild steel (ST3S) strip under axial tension at the onset of plastic flow. The fringe shown in fig. 1 takes place in the region, in which the stress state has been reached causing plastic flow. A point on the load — displacement curve corresponding to this state is marked

Fig.1.

with „*a*" in fig. 2. The obtained fringe can be treated as a trace of slipline in the local neck as shown in fig. 3. It is possible to find a statically admissible stress field corresponding to such a deformation mechanism, thus obtaining a simple and well known exact solution.

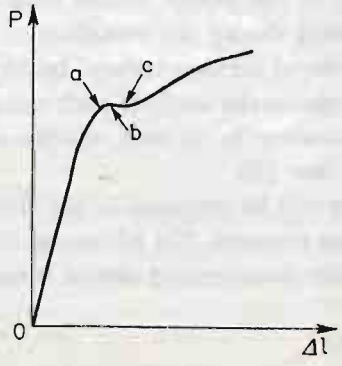

Fig. 2.

The fact that ST3S steel behaves in the investigated range approximately as an elastic — ideally plastic material can be utilized for investigating failure modes in notched metal strips in plane stress. An element well known both from theoretical ([1], [5]) and experimental [2] studies is a strip weakened by arrays of holes as shown in fig. 4. Such an element has been chosen as an example for demonstrating the presented method. An attempt is made to verify experimentally the failure mechanism shown in fig. 5 (denoted further as A) used for the upper bound assessment of the limit load of the strip, cf. among others, [1, 5]. Two series of tests were made, both on steel strips of thickness $g = 2$ mm weakened by holes of diameter $d = 10$ mm and spaced at $t = 35$ mm ($t/d = 3.5$). The distance s between the arrays of holes was $s = 15, 18, 21, 24, 27, 30$ mm and $s = 10.5, 14, 17.5, 21, 24.5$ mm for the first and the second series, respectively.

Cross line gratings of density 40 lines/mm were printed photographically on all the strips. Specimens were subjected to axial tension in the universal testing machine INSTRON/1251 with constant velocity of the longitudinal displacement 0.1 mm/min. The

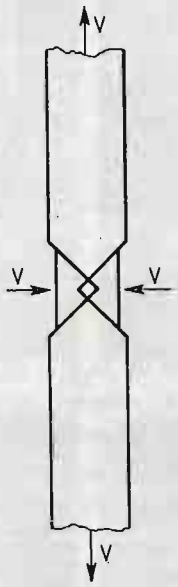

Fig. 3.

load — displacement curve was plotted automatically during the loading process. At the same time the photographs of the moiré patterns were taken, each photograph corresponding to a certain point on the load — displacement curve. The tests enabled us to make the following remarks:

A characteristic load — displacement curve, as shown in fig. 2, was obtained for all the strips tested. The process of formation of plastic zones for $s = 21$ mm ($s/t = 0.6$) is shown in fig. 6. Thin fringes appearing succesively during the test will be treated, as previously (see fig. 1), as a manifestation of failure mechanism of a given element. Photographs shown in fig. 6 a, b, c correspond to the points a, b, c marked on the load — displacement curve shown in fig. 2. It is a typical process of reaching the limit state in steel

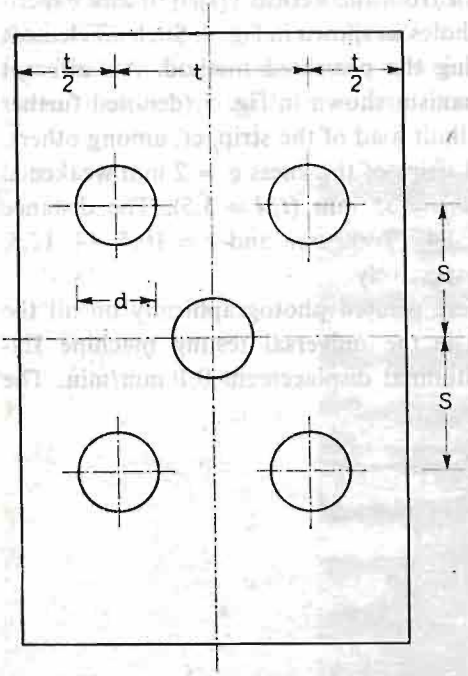

Fig. 4.

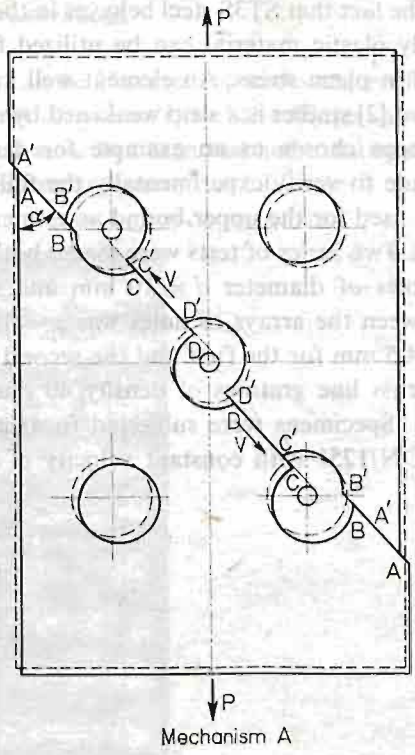

Fig. 5.

strips revealed in all the test specimens up to $s = 21$ mm. Photographs for $s = 10.5$ mm ($s/t = 0.3$) and $s = 14$ mm ($s/t = 0.4$), selected as examples, are shown in fig. 7a, b, respectively. After the formation of a mechanism such as in fig. 6c mutual displacements of separate parts of the strip were observed as rapid changes in the moiré patterns. Some dissimilarities of the obtained mechanism as compared with the mechanism A shown in fig. 5, can be seen.

The generation of the failure mechanism for $s = 24.5$ mm ($s/t = 0.7$) is shown in fig. 8. Photographs in fig. 8a, b correspond to the points a, c on the load — displacement curve (fig. 2), respectively. At the same load level two mechanisms can be seen to be present. The first one consists of a local necking (see fig. 3) along the horizontal axes of lower and upper rows of holes, while the second is similar to that previously described (see fig. 6a).

For $s = 27$ mm ($s/t = 0.77$) the formation of each mechanism can be clearly distinguished. During the loading, the mechanism similar to that of fig. 8a appears first. The other one appears for considerably increased load. For $s = 30$ mm ($s/t = 0.86$) only the mechanism shown in fig. 8a is present. Thus, for $s \geqslant 27$ mm the mechanism shown in fig. 8a and fig. 3 is valid. The distance $s = 24.5$ mm ($s/t = 0.7$) is thus the so — called optimum value s_{opt} [5]. When $s = s_{opt}$ the limit state can be reached following any of the described patterns.

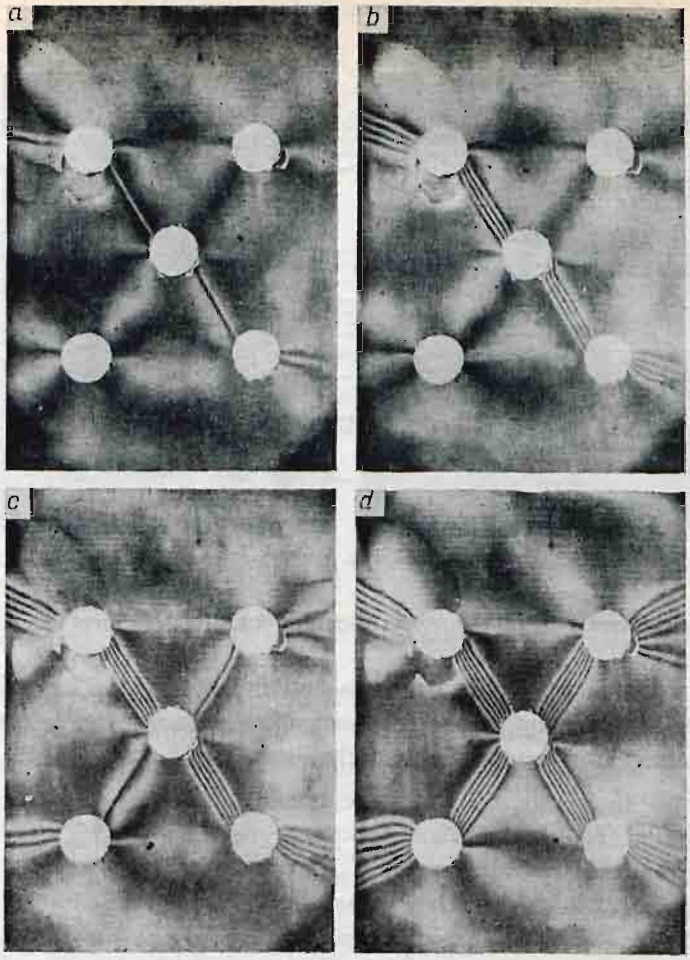

Fig. 6

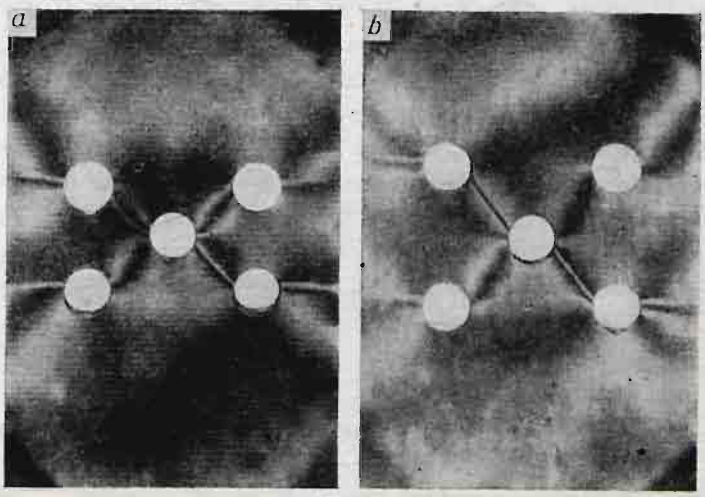

Fig. 7.

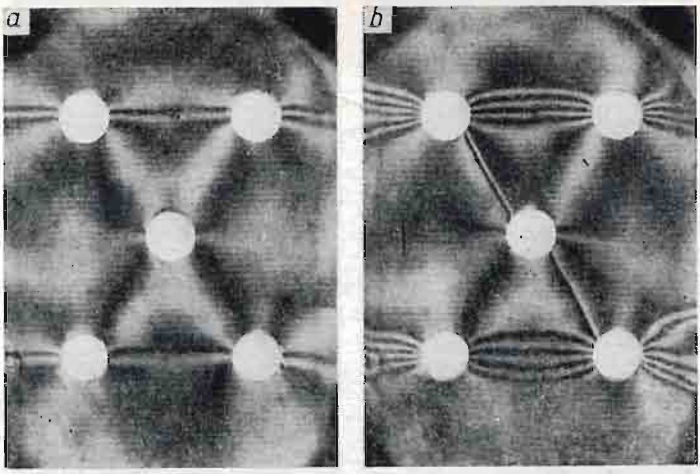

Fig. 8.

3. Theoretical analysis of the experimentally obtained failure mechanism

The failure mechanisms obtained in tests and shown in fig. 6 can be interpreted in two ways as it is shown in fig. 9a, b. The mechanism shown in fig. 9a can be considered as the initial stage of formation of the mechanism shown in fig. 9b. In both cases the

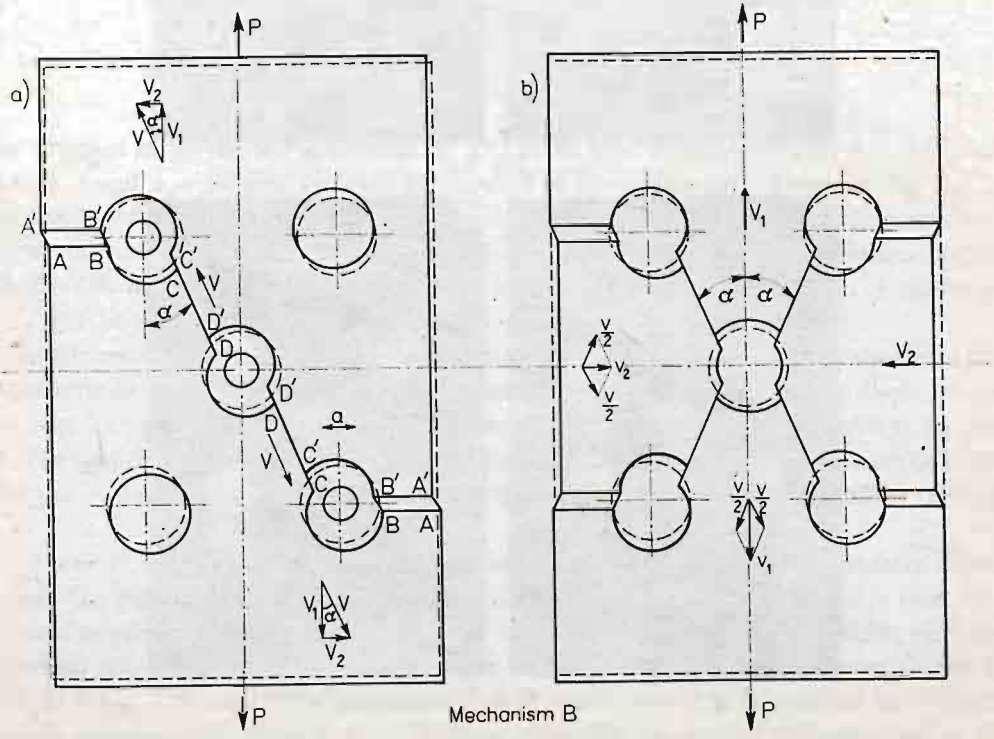

Fig. 9. a, b

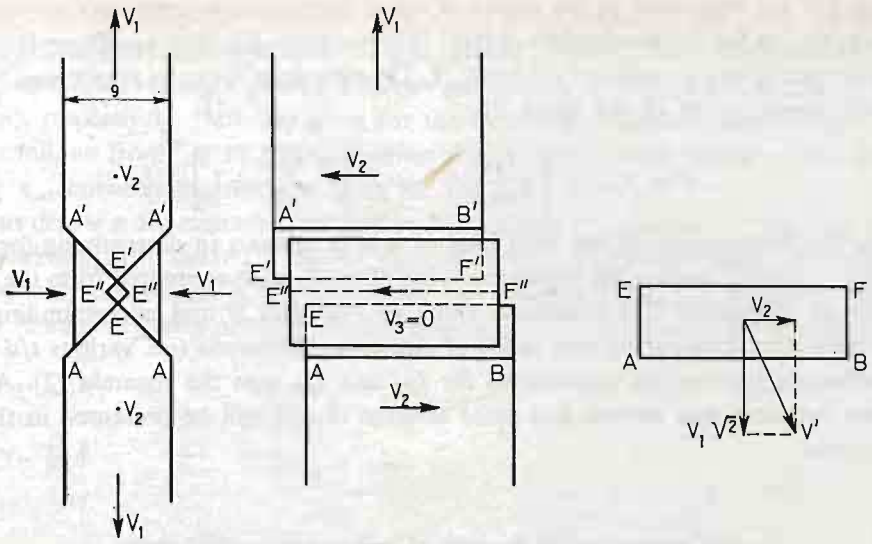

Fig. 9. c, d, e

virtual work principle furnishes the same upper bound to the limit load. Thus, only the mechanism shown in fig. 9a (denoted further as *B*) will be analysed. The failure, interpreted as the development of large plastic strains consists in mutual displacement of both parts of the strip parallel to the line inclined at an angle to the vertical axis. Such a displacement is generated along *CD* — lines. Along these lines the tangential stress has to be equal to the yield stress at pure shear, e.g. to $k = \sigma_{pl}/2$ according to the Coulomb — Tresca yield criterion. Along the lines *AB* a different mode, consisting in a combined local necking (see fig. 9c) and mutual horizontal displacement (see fig. 9d) takes place. Lines *AA'* and *BB'* are parallel to the lines *CD*, thus ensuring the continuity of deformation under combined action of both described mechanisms. Along the lines *AB* the yield stress at pure shear $k = \sigma_{pl}/2$ is also present, but its direction depends on the resultant velocity of the mutual displacements of the parts of the strip.

With the distance *s* and the angle α known, upper bound to the limit load is obtained by equating the increment of external work done to the increment of the work dissipated by internal forces in the shearing planes. Assuming that both parts of the strip move along the lines *CD* with the relative velocity $2v$, the velocity of their mutual displacement in the AEFB plane (fig. 9d, e) will be $v' = v\sqrt{2\cos^2\alpha+\sin^2\alpha}$. Thus the following virtual work equation is obtained:

$$P \cdot 2v\cos\alpha = 2\left[\frac{1}{2}\sigma_{pl}\cdot g\cdot l_{CD}\cdot 2v+\frac{1}{2}\sigma_{pl}\cdot 4\cdot g\frac{\sqrt{2}}{2}\cdot l_{AB}\cdot v\sqrt{2\cos^2\alpha+\sin^2\alpha}\right] \qquad (1)$$

where l_{AB}, l_{CD} denote the lengths of the lines *AB* and *CD*, respectively and *g* is the thickness of the element.

Given a certain configuration of holes, the angle α can easily be determined. Then, the minimum value of the force *P* can be computed from equation (1) by assuming such *CD* lines configuration which their minimum length. The latter condition is fulfilled when

the lines CD are tangential to the circles of equal diameter a located concentrically with the holes, e.g. as for the mechanism A (fig. 5) taken from [5]. This condition is also confirmed by tests as can be seen in fig 6 or fig. 7. The equation (1) can be rearranged to enable the direct computation of the force P:

$$P = \sigma_{pl} \cdot g \cdot \left[\frac{l_{CD}}{\cos \alpha} + l_{AB} \cdot 2 \cdot \sqrt{\frac{tg^2 \alpha}{2} + 1} \right]. \tag{2}$$

Thus the computation of the limit load of a strip consists in determining for a given set of d, t, s such an angle α for which the value of the force P computed from the formula (2) is at its minimum. The minimum value of the force P and corresponding angles α have been computed for various ratios of elements dimensions (i.e. various t/d and s/t) by substituting appropriate expressions for l_{AB} and l_{CD} into the formula (2). A simple computer program was written and some selected results will be presented in the following section.

4. Comparison of theoretical and experimental results

One of the problems connected with the estimation of the limit load of strips weakened by several rows of holes is the determination of the least distance $s = s_{opt}$ (see fig. 4) between the rows for which the load — carrying capacity of a strip is equal to the load — carrying capacity of a strip weakened by only one row of holes. The limit load of such a strip is given by the formula:

$$P = 2 \cdot \sigma_{pl} \cdot g \cdot (t - d). \tag{3}$$

Theoretical solution to this problem obtained on the basis of both statically admissible stress field (lower bound) and kinematically admissible collapse mechanism A (fig. 5) (upper bound) was presented in [5]. The $s_{opt}(t$ vs. t/d diagrams are shown in fig. 10.)

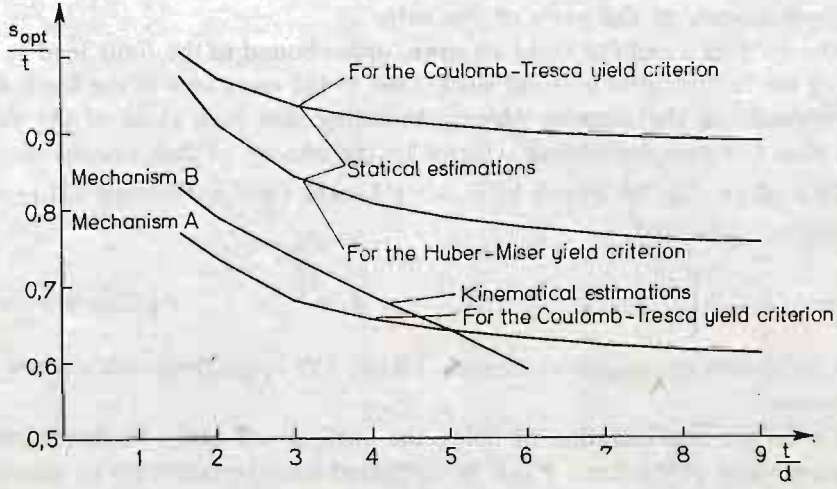

Fig. 10.

Statical (upper) estimations of the ratio s_{opt}/t, taken from [5], are given for the Coulomb — Tresca yield criterion and for the Huber — Mises one. Kinematical (lower) estimations of this ratio are given for failure mechanism A (fig. 5) and B (fig. 9) (curves A and B), respectively. Both are given for the Coulomb — Tresca yield criterion.

As it follows from fig. 10, the mechanism B gives better lower bound on the optimum distance s_{opt} between the rows of holes for $t/d < 5$.

Let us define a dimensionless factor $f = P/P_m$ where P is the load — carrying capacity of the weakened strip (as in fig. 4) and P_m is the load — carrying capacity of a strip weakened by only one row of holes. The factor f is called (see e.g. [1]) the load — carrying capacity increment factor although in our tests it was less than unity for the whole range of load.

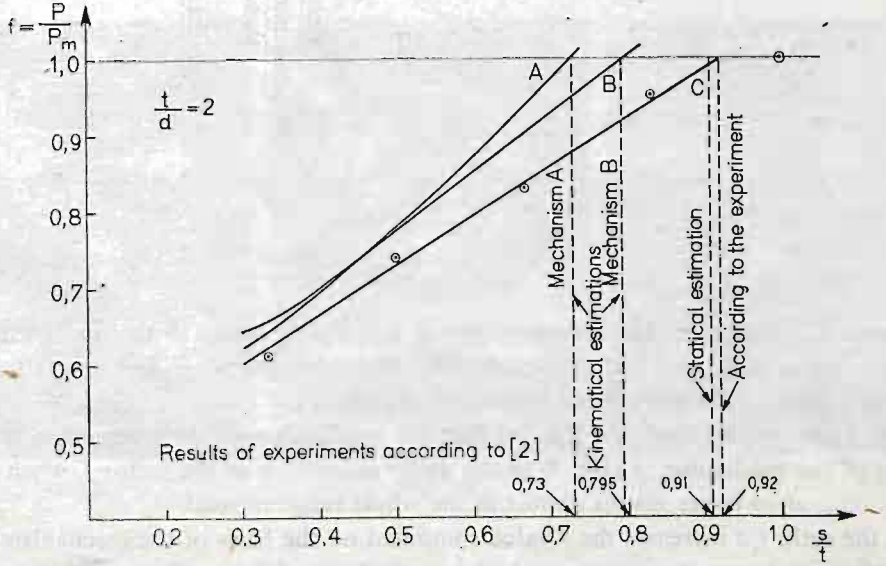

Fig. 11.

Theoretically obtained f vs. s/t diagrams plotted for $t/d = 2$ are presented in fig. 11. The ratio $t/d = 2$ was chosen so as to make the comparison of our results with those obtained by Dietrich [2]. The curves A and B are obtained for mechanisms A and B, respectively, the curve C was obtained in [2] by statical investigation of strips made of PA2 aluminium alloy.

Here we can see, as in fig. 10, that the application of experimentally obtained mechanism B considerably narrows the gap between kinematical and statical bounds. At the same time the lower estimation of the optimum value s_{opt} (for $f = 1$ we have $s/t = 0.795$ instead of 0.73) is closer to the obtained experimentally ratio $s/t = 0.92$.

The experiments also confirm the correctness of using the mechanism B for the estimation of s_{opt}. For the strips tested, e.g. for $t/d = 3.5$ (see fig. 12), the lower estimation of the optimum distance between the arrays of holes gives for theoretically assumed

mechanism A $s_{opt} = 23.4$ mm ($s/t = 0.67$) and for experimentally obtained mechanism B (fig. 9) $s_{opt} = 24.9$ mm ($s/t = 0.71$), both for the Coulomb — Tresca yield criterion. The upper estimation for the Huber — Mises yield criterion is $s_{opt} = 28.8$ mm ($s/t = 0.82$).

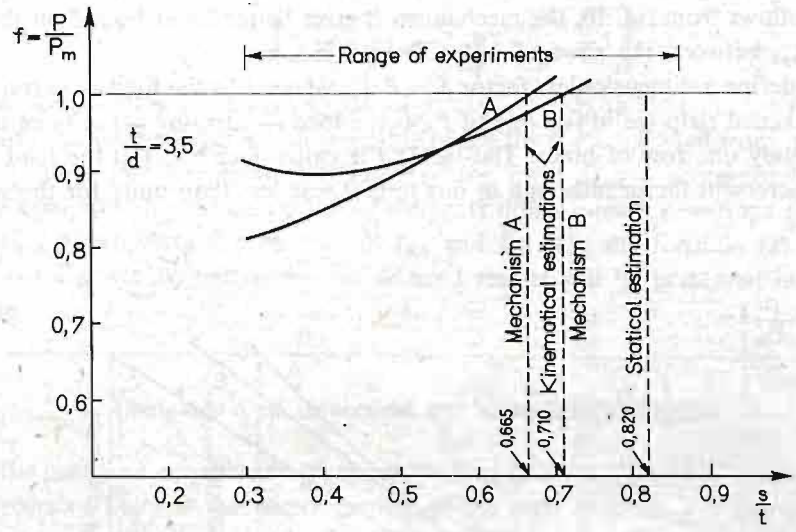

Fig. 12.

The value s_{opt} computed for the mechanism B is not only closer to the upper estimation but also agrees very well with experimentallyobtained distance $s = 24.5$ mm ($s/t = 0.71$), what has already been pointed out at the end of section 2.

It is worth noting (see also fig. 11) that the application of the mechanism B (fig. 9) instead of the mechanism A (fig. 5) to the upper estimation of the factor f, when $t/d \leqslant 2$ for $s < s_{opt}$, gives better results almost in the whole range of load.

As the ratio t/d increases the f value computed on the basis of the mechanism B tend to be relatively larger than those computed on the basis of the mechanism A. An example of this tendency is shown in fig. 12 for $t/d = 3.5$, i.e. the ratio for which the tests were performed. In this case only in the small interval ($s/t > \sim 0.57$) curve B lies below curve A. Nevertheless it has to be stressed that for the whole range of s/t ratio, namely $0.3 \leqslant s/t \leqslant 0.7$, the formation of the mechanism B has been observed. For $t/d > 5$ (see also fig. 10) the application of the mechanism B (fig. 9) gives greater values of f than the application of the mechanism A (fig. 5) in the whole range of s/t ratio. The statical evaluation of the factor f resulting from our experiments is absent from the diagram (fig. 12) due to insufficiently numerous set of specimens tested. The ST3S mild steel used in our investigations is relatively nonhomogeneous material and gives considerable scatter of results.

5. Final remarks

The main purpose of this work is a presentation of a simple method for evaluation of the failure modes in notched plane metal elements. The application of the moiré method

in several tests has given a clear answer: for the presented examples (fig. 6 - 8) it is the experimentally obtained mechanism *B* (fig. 9) that is appropriate. Its application results in narrowing of the gap between the statical and the kinematical solutions.

It cannot be, of course, ruled out that for ratios of element dimensions (different s/t and t/d ratios) a different failure mode, possibly the mechanism *A* (fig. 5), would have been obtained. The moire method remains, however, a suitable tool in an adequately equipped laboratory to arrive at reliable results by way of simple tests.

Finally, it is worth pointing out that the moiré method is also suitable for the examination of plastic zones propagation in plane elements of arbitrary shapes. Initial stages of these zones have already been shown in fig. 6a, b, c, d and in fig. 8b. Their further development is presented in fig. 13a, b, c.

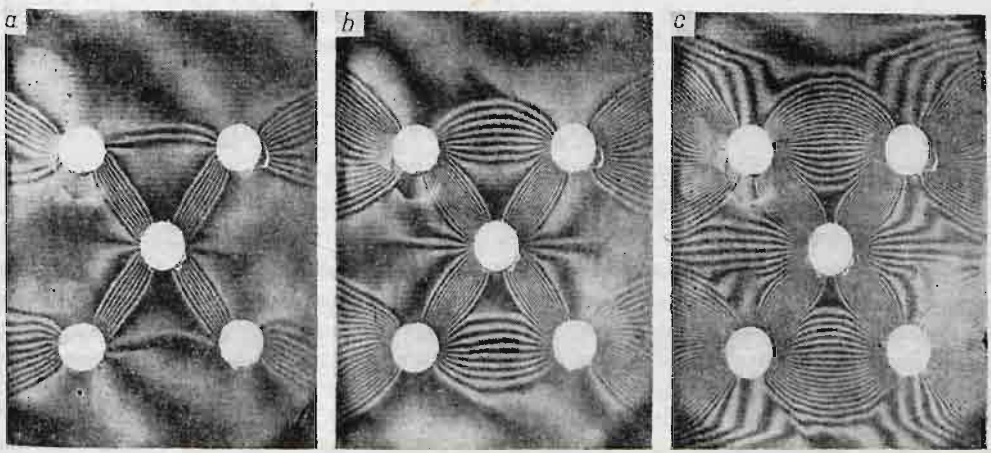

Fig. 13

Bibliography

1. L. DIETRICH, J. MIASTKOWSKI, W. SZCZEPIŃSKI:, *Nośność graniczna elementów konstrukcji*, PWN, Warszawa 1970.
2. L. DIETRICH, *Projektowanie plastyczne a wytrzymałość zmęczeniowa pasma z otworami*, Rozpr. Inż., T. 25, z. 4, Warszawa 1977, s. 659 - 670.
3. P. JASTRZĘBSKI, *Limit Load of Steel Strips with Circular Holes*, Bull. Acad. Polon. Sci., Sér. Sci. Techn., Vol XVIII, N 6, 1970.
4. J. KAPKOWSKI, *Propagacja obszarów plastycznych w warunkach płaskiego stanu naprężeń*, Prace Naukowe P.W. — Mechanika z. 50, Warszawa 1976.
5. W. SZCZEPIŃSKI, *Projektowanie elementów maszyn metodą nośności granicznej*, PWN, Warszawa 1968.
6. P. JASTRZĘBSKI, J. KAPKOWSKI, J. WĄSOWSKI, S. WICHNIEWICZ, K. PATORSKI, *Zastosowania metody mory do badania elementów konstrukcji*, Skrypt wykładów, Komitet Mechaniki PAN, Warszawa-Jabłonna 1981.

Р е з ю м е

ПРИМЕНЕНИЕ МЕТОДА МУАРА ДЛЯ АНАЛИЗА КИНЕМАТИЧЕСКИХ МЕХАНИЗМОВ РАЗРУШЕНИЯ МЕТАЛИЧЕСКИХ ПОЛОС

В статьи представляется способ использования метода муара для однозначного определения кинематического механизма пластического разрушения элементов с нарезами, которые находятся в плоском напряжённом состоянии. В работе показаны примеры экспериментальных исследований проведенных на стальных полосах с пятью круговыми отверствиями (рис. 4) расставленными в трёх рядах при переменным их размещении (10 вариантов). Указан факт, что полученый экспериментально механизм (рис. 9) отличается от прежде примененного для конкретных полос (рис. 5). Этот механизм описывается теоретически. Констатируется, что его применение позваляет на лучшую оценку верхней границы (кинематической) предельной нагрузки, чем применяемый до сих пор для практически важных пропорций размеров. Достоинством этого метода является возможность наблюдения кинематического механизма пластического разрушения (рис. 6 - 8) почти от начала его реализации и явлений связанных с его существованием. Кроме того существует возможность испытания развития области пластических деформаций соразмерно с приростом нагрузки.

S t r e s z c z e n i e

ZASTOSOWANIE METODY MORY DO ANALIZY KINEMATYCZNYCH MECHANIZMÓW ZNISZCZENIA PASM METALOWYCH

W artykule przedstawiono sposób wykorzystania metody mory do jednoznacznego określania kinematycznych mechanizmów zniszczenia elementów z karbami znajdujących się w płaskim stanie naprężenia. Podano przykłady badań doświadczalnych przeprowadzonych na pasmach stalowych z pięcioma otworami kolistymi (rys. 4) rozmieszczonymi w trzech rzędach, przy zmiennym ich rozstawieniu (10 wariantów). Wskazano na to, że otrzymany doświadczalnie mechanizm (rys. 9) różni się od stosowanego poprzednio [1, 5] dla takich pasm (rys. 5), a opisany teoretycznie daje dla praktycznie ważnych proporcji wymiarów lepsze oszacowanie górnej oceny (kinematycznej) nośności granicznej niż dotychczas stosowany. Zaletą tej metody jest możliwość obserwacji kinematycznego mechanizmu zniszczenia (rys. 6 - 8) niemal od początku jego realizacji oraz zjawisk związanych z jego powstaniem. Istnieje też możliwość badania. rozwoju obszarów plastycznych w miarę wzrostu obciążenia (rys. 6, 8, 13).

Praca została złożona w Redakcji dnia 15 marca 1983 roku

Praca wykonana w ramach Problemu Węzłowego 05.12.